Electronic and magnetic properties of $La_4BaCu_{5-x}Mn_xO_{13+\delta}$

1998 J. Phys.: Condens. Matter 10 8477

(http://iopscience.iop.org/0953-8984/10/38/008)

J. Phys.: Condens. Matter **10** (1998) 8477–8484. Printed in the UK PII: S0953-8984(98)94058-9

Electronic and magnetic properties of $La_4BaCu_{5-x}Mn_xO_{13+\delta}$

G D Liu†, G C Che, Z X Zhao, S L Jia, S Q Guo, Y Z Zhang, H Chen, F Wu and C Dong

National Laboratory for Superconductivity, Institute of Physics, Chinese Academy of Sciences, Beijing 100080, People's Republic of China

Received 12 May 1998

Abstract. Perovskite $La_4BaCu_{5-x}Mn_xO_{13+\delta}$ has been synthesized and its structure, electronic and magnetic properties have been investigated. Results indicate that: (1) a metal–insulator transition is observed due to the substitution of Cu by Mn, (2) the temperature dependence of resistivity can be described by a three-dimensional variable-range-hopping conduction due to the hopping between localized states near the Fermi energy level in an inhomogeneous medium and (iii) their magnetic susceptibility obeys well the Curie–Weiss Law.

1. Introduction

Transition metal oxides with perovskite or perovskite derived structure have displayed varieties of interesting electronic transport and magnetic properties. Since the discovery of the first high temperature cuprate superconductor (HTSC) by Bednorz and Müller [1], study of the colossal magnetoresistance (CMR) effect in hole-doped manganese oxides has seen a revival in recent years.

These two large topics, HTSC and CMR, have many similarities. HTSC primarily involves cuprate compounds. The CMR effect appears mainly in manganese compounds. Both HTSCs and CMR manganese oxides have their corresponding antiferromagnetic (AFM) parent insulator. With increasing hole doping the cuprate parents transform from AFM insulator into completely diamagnetic HTSC [2], and the manganese compounds become ferromagnetic metals [3]. In other words, both magnetic and metal–insulator (MI) transitions occur in these two systems. An optimum carrier concentration was observed in both HTSC and CMR systems. For HTSC, T_c is maximum at about 0.15 hole doping [4]. For CMR compounds, T_C reaches its maximum at about 0.33 doping [5]. Also Cu and Mn ions with mixed valency state are clearly important to these two systems. Throughout they are all strong correlation systems. It is particularly interesting that evidence of the existence of polarons in these two systems was found by G M Zhao *et al* [6, 7]. Furthermore, it is found almost without exception that substitutions at Cu or Mn sites all lead to the fall of the superconducting critical temperature T_c or ferromagnetic Curie temperature T_C. The above similarities make some people speculate that the HTSC and CMR effects maybe have similar or even the same origin.

† Corresponding author: Dr Guodong Liu, National Laboratory for Superconductivity, Institute of Physics, Chinese Academy of Sciences, PO Box 603, Beijing 100080, People's Republic of China. E-mail address: gdliu@ssc.iphy.ac.cn.

0953-8984/98/388477+08$19.50

In this regard, Cu and Mn are two peculiar elements and it is very possible that Mn ordering or disordering substitutions at Cu sites in some HTSC-related material could reveal some significant information to us.

Some studies of Mn substitution for Cu sites in HTSC compounds have already been carried out [8–12]. It is found that Mn substitution of Cu sites decreases T_c and induces the MI transition. Research on the metal–insulator (MI) transition is very significant to search for new HTSC directions and could reveal the mechanism of high temperature superconductivity.

It is well known that perovskite-related $La_4BaCu_5O_{13+\delta}$ was, at an early stage, considered by Bednorz and Müller [1] as a potential material for superconductivity. This compound is a good metallic conductor and is in fact not superconducting. We found that the compound undergoes a metal–insulator transition with the substitution of Cu by Mn. In this paper, structural aspects, electronic and magnetic properties of $La_4BaCu_{5-x}Mn_xO_{13+\delta}$ was investigated.

2. Experiment

The samples were prepared by the conventional solid state reaction route. Stoichiometric amounts of high purity powders of La_2O_3, $BaCO_3$, CuO and MnO_2 were mixed thoroughly, and calcinated at 925 °C for 20 h, then the products were reground and pelletized, and sintered again at 1000 °C for 40 h before slowly cooling to room temperature.

X-ray diffraction (XRD) analysis was carried out by an M 18X-AHF diffractometer using Cu Kα radiation. Lattice parameters were calculated by FINAX and LAZY programs.

The resistivity measurements were performed on a $10 \times 4 \times 2$ mm^3 rectangular bar cut from the samples by a standard four-probe method, using silver paste as contacts. The resistance measurements with varying current density at different temperature show a well defined Ohm law in each case. The data were collected from room temperature down to about 5 K. The temperature was monitored by a calibrated Rh–Fe probe embedded in the copper mount over which the sample was fitted with vacuum grease. Great care was taken to avoid influence of thermal hysteresis on the measurements.

The DC magnetization was measured using about 200 mg samples with a $6 \times 3 \times 3$ mm^3 size on a MPMS-5 type of SQUID magnetometer from 5 K up to 315 K under an applied field of 5000 G. Measurements were performed under zero field cooling (ZFC). Owing to the relatively large quantity of the sample an overall measurement precision of about 1% could be obtained for the susceptibility.

3. Results and discussion

3.1. Structural information

The structure of $La_4BaCu_5O_{13+\delta}$, which has been determined by powder neutron diffraction, is closely related to that of perovskite with a tetragonal cell of $a = 8.647$ Å $\approx \sqrt{5}a_p$ and $c = 3.859$ Å $\approx a_p$ [13], where a_p is the edge length of the cubic perovskite unit cell. The space group (SG) is $P4/m$. The $[Cu_5O_{13}]$ framework is built up from corner-sharing CuO_5 pyramids and CuO_6 octahedra forming hexagonal tunnels and perovskite cages where the lanthanum and barium ions are located in an ordered manner. The Ba^{2+} ions are located in the perovskite tunnels whereas the La^{3+} ions occupy the hexagonal tunnels. In this structure, one special feature of the $[Cu_5O_{13}]$ network is the geometry of the hexagonal tunnels, which is rather different from the ideal model derived from the stoichiometric perovskite structure.

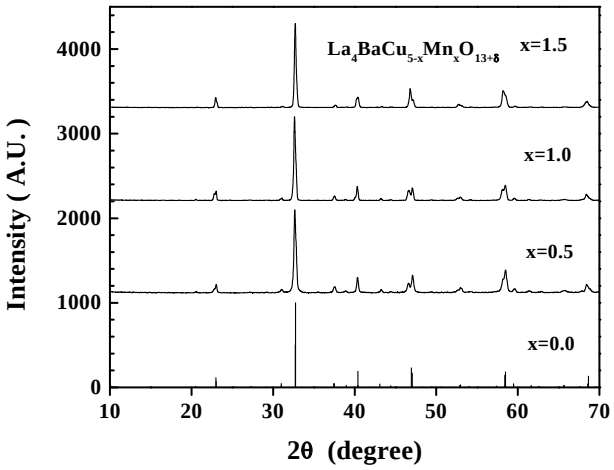

Figure 1. XRD patterns of $La_4BaCu_{5-x}Mn_xO_{13+\delta}$ samples with $x = 0.0$, 0.5, 1.0, 1.5. The pattern with $x = 0.0$ is from the calculated result.

Figure 1 shows XRD patterns of some typical $La_4BaCu_{5-x}Mn_xO_{13+\delta}$ samples and the XRD pattern calculated using the structural parameters of $La_4BaCu_5O_{13+\delta}$ in [13]. Experimental results indicate that single-phase samples for $La_4BaCu_{5-x}Mn_xO_{13+\delta}$ can be obtained when $0 \leqslant x \leqslant 1.5$, and the substitution of Mn for Cu is random. The lattice parameters for $La_4BaCu_{5-x}Mn_xO_{13+\delta}$ are listed in table 1.

Table 1. Lattice parameters of $La_4BaCu_{5-x}Mn_xO_{13+\delta}$.

x	a (Å)	c (Å)	V (Å^3)
0.0	8.6358	3.8629	288.08
0.5	8.6782	3.8603	290.73
1.0	8.6855	3.8586	291.08
1.5	8.6583	3.8706	290.16

3.2. Electronic transport behaviour

Figure 2 shows variation of the resistivity as a function of temperature from room temperature down to about 4.2 K for $La_4BaCu_{5-x}Mn_xO_{13+\delta}$ ($x = 0.0$, 0.5, 1.0, 1.5). Without Mn substitution, the sample $La_4BaCu_5O_{13+\delta}$ (pure La415) show good metallic behaviour. It is consistent with the result reported previously by C Michel *et al* [14]. Above about 150 K, the curve can be fitted by a straight line. The deviation from linearity at low temperature is attributed to the influence of defects and especially to oxygen vacancies. All our Mn-substituted samples exhibit a semiconductor-like temperature dependence of resistivity. This suggests that the Mn substitutions for Cu induce a metal–insulator (MI) transition beyond a substitution range of about 10%. Moreover, resistivity values of samples increase with increasing Mn content at any temperature. We note the resistivity of all Mn-substituted samples increases very rapidly with decreasing temperature below 40 K.

Figure 3 shows the resistivity at room temperature 290 K, ρ_{290}, as a function of dopant concentration of Mn. With increasing Mn content x, ρ_{290} increases not linearly but more

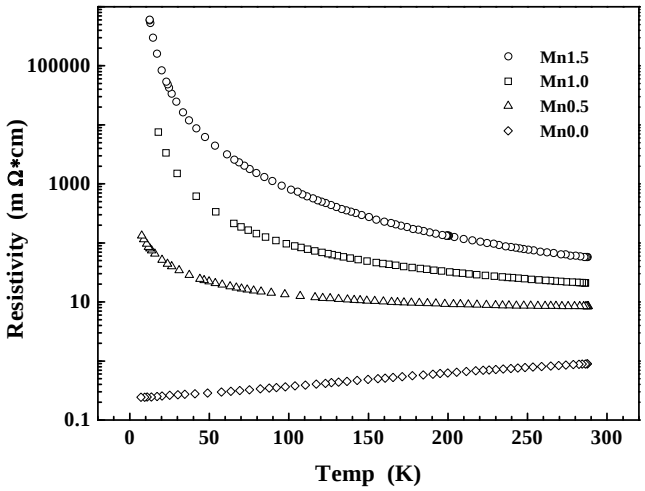

Figure 2. Variation of the resistivity as a function of temperature from room temperature down to about 4.2 K for $La_4BaCu_{5-x}Mn_xO_{13+\delta}$ ($x = 0.0$, 0.5, 1.0, 1.5).

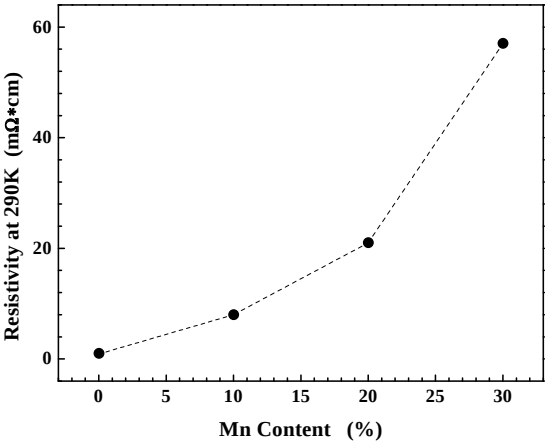

Figure 3. Variation of the resistivity at 290 K as a function of Mn content for $La_4BaCu_{5-x}Mn_xO_{13+\delta}$ with $x = 0.0$, 0.5, 1.0, 1.5. Note: in figures 3 and 6 the content values $x = 0.0$, 0.5, 1.0, 1.5 are changed to the Mn content (%) of Mn substitution for Cu as 0, 10, 20, 30, respectively.

rapidly. This result implies that the impurity-scattering mechanism is invalid in explaining the x doping dependence of ρ_{290} for the Mn-substituted samples.

Analyses of the resistivity data reveal that the semiconductor-like behaviour of Mn-substituted samples cannot be well described by a thermally activated mechanism. Instead, they can be well described by a variable-range-hopping (VRH) conduction process between localized states near the Fermi energy. The general form of a VRH conduction formula [15] is:

$$\rho(T) = \rho_0 \exp\left(\frac{T_0}{T}\right)^{\alpha} \tag{1}$$

where T_0 is the Mott characteristic temperature, and

$$\alpha = \frac{n+1}{n+D+1}. \tag{2}$$

D is here the dimensionality of the hopping process, and n describes the energy dependence of the density of states $N(E_F)$ in the vicinity of the Fermi energy, which behaves like $N(E_F) \sim (E - E_F)^n$. For an energy-independent density of states $n = 0$, equation (2) leads to a Mott–Davis variable-range-hopping case of $\alpha = 1/3$ in two dimensions, and $\alpha = 1/4$ in three dimensions. The mean hopping distance $R_{hop}(T)$, the mean hopping energy $E_{hop}(T)$ and T_0 are given as follows [16]:

$$R_{hop}(T) = \frac{3}{8}a\left(\frac{T_0}{T}\right)^{\frac{1}{4}} \tag{3a}$$

$$E_{hop}(T) = \tfrac{1}{4}k_B T^{\frac{3}{4}} T_0^{\frac{1}{4}} \tag{3b}$$

$$T_0 = 18/[k_B N(E_F) a^3]. \tag{3c}$$

Here, $N(E_F)$ has the same meaning as in the above text, while a is the localization length of states near the Fermi energy level.

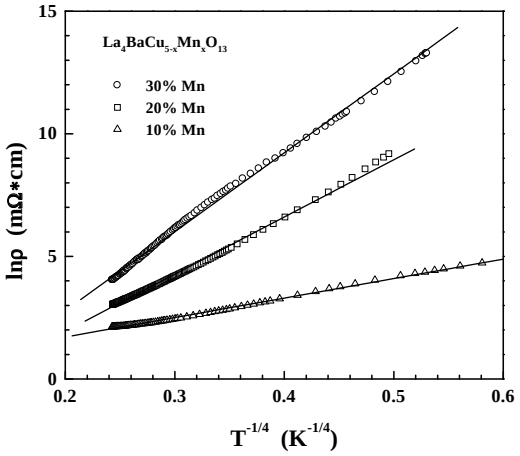

Figure 4. $\ln\rho$ against $T^{-1/4}$ plots for $La_4BaCu_{5-x}Mn_xO_{13+\delta}$ ($x = 0.5$, 1.0 and 1.5) samples.

We used formula (1) to fit the measured resistivity data for the Mn-substituted samples. We found that these data can be reasonably well fitted by three-dimensional VRH conduction. Figure 4 shows the data plotted as $\ln(\rho)$ against $T^{-1/4}$ together with the least squares fitted line. The fitted $R_{hop}(T)$, $E_{hop}(T)$ at 10 and 300 K, T_0 and $N(E_F)$ under the reasonable assumption of $a = 10$ Å are listed in table 2. Thus, the observed semiconductor-like behaviour should be attributed to three-dimensional VRH conduction between localized states near the Fermi energy. The slight deviations from linearity of the curves in figure 4 may be related to the magnetic scattering from Mn localized moments. Comparing the good metallic conduction in pure La415 with its itinerant carriers against the VRH conduction in Mn-substituted samples with localized carriers, it can be deduced that the MI transition in La415 compounds with Mn doping originates from hole localization induced by Mn doping. Here the behaviour of Mn is quite unlike in $La_{1-x}A_xMnO_3$ (A = Ca, Sr, Ba) perovskites in which ordering of Mn induces metallic transport behaviour. In $La_4BaCu_{5-x}Mn_xO_{13+\delta}$

compounds, the charge of Mn can be reasonably thought of as +3 [17]. Since the sintered La415 samples contain very little excess oxygen addition of Mn in La415 lowers rapidly the concentration of holes. As a result, resistivity must increase with rising Mn content in the $La_4BaCu_{5-x}Mn_xO_{13+\delta}$ system. Further reasons for hole localization induced by Mn doping may include: (1) the holes are localized by Mn ions, which is reasonable considering the relative 3d energy levels of Mn and Cu; (2) random substitution of Mn for Cu induces Anderson localization; (3) oxygen vacancies enhance the localization of carrier's particularly at low temperature.

Table 2. The fitted parameters of magnetic and electronic transport properties for $La_4BaCu_{5-x}Mn_xO_{13+\delta}$ samples.

x	C ($\times 10^{-3}$) (emu K G^{-1} g^{-1})	p_{eff} (μB)	θ (K)	T_0 (K)	E_{hop} (10 K) (meV)	R_{hop} (10 K) (Å)	$N(E_F)$ (eV^{-1} cm^{-3})
0.0	—	—	—	—	—	—	—
0.5	1.24	11.0	−15.48	3981	0.96	16.8	5.25×10^{22}
1.0	2.14	10.22	−29.41	295 540	2.8	49.2	7.07×10^{20}
1.5	3.28	10.33	−47.73	1 077 443	3.9	67.9	1.94×10^{20}

3.3. Magnetic properties

Shown in figure 5 is the variation of magnetic susceptibility $\chi = M/H$ under a field of 5000 G for the above four samples with temperature. In particular no magnetic ordering has been found over the measured temperature range from 315 K down to 5 K. As reported by Torrance *et al* [18], the mass susceptibility for pure La415 sample is very weak. It decreases slightly with increasing temperature up to 250 K and then becomes nearly temperature independent. The molar susceptibility χ_m values ($\chi_m = (110\text{–}120) \times 10^{-5}$ emu at room temperature) are too high to be interpreted as a Pauli paramagnetism of an electron gas. Accordingly some strong electron correlation is assumed in this compound. The main features of the curves in figure 5 for Mn-substituted samples are (1) the presence of a sizable constant susceptibility term near room temperature; (2) an increasing Curie-like term as the Mn content increases; (3) a gradually developing kink around 100 K with increasing Mn content.

The data are well fitted by the Curie–Weiss law as follows:

$$\chi = \chi_0 + \frac{C}{T - \theta} \tag{4a}$$

$$C = \frac{N p_{eff}^2 \mu_B^2}{3k_B}. \tag{4b}$$

Here, χ_0 is the temperature independent susceptibility term. C is the Curie constant. θ is the Curie–Weiss temperature. N is the concentration of Mn in $La_4BaCu_{5-x}Mn_xO_{13+\delta}$ and p_{eff} their effective moment. This further suggests that carriers in Mn doped samples are localized. This conclusion is supported by the semiconductor-like resistivity behaviour. The fitted parameters C, p_{eff} and θ are listed in table 2.

From figure 5, the Mn-substituted La415 compounds show essentially paramagnetic behaviour above 5 K. No observable magnetic ordering is again evidence of random Mn distribution in lattice. Clearly though the fitted effective moment values $\sim 10\ \mu_B$ for Mn are too high to be explained by a simple spin-only effective moment of the Mn^{3+} ion. The

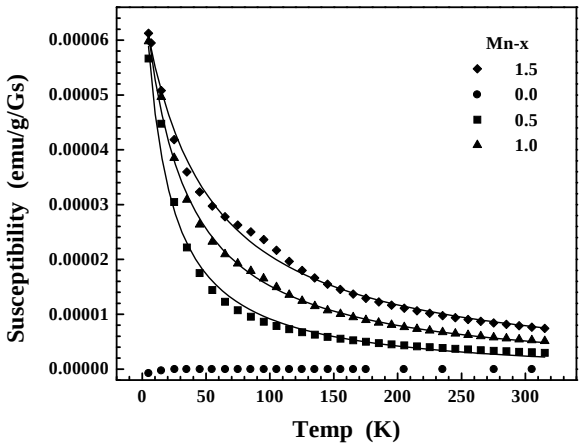

Figure 5. Raw-data susceptibility of $La_4BaCu_{5-x}Mn_xO_{13+\delta}$ ($x = 0.0$, 0.5, 1.0 and 1.5) samples under 5000 G in zero field cooling mode. The fitted lines using the Curie–Weiss law are also shown.

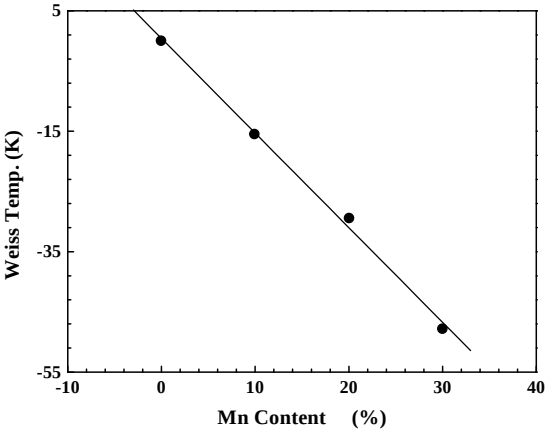

Figure 6. Curie–Weiss temperature against Mn content for the $La_4BaCu_{5-x}Mn_xO_{13+\delta}$ system.

theoretically effective moment of Mn^{3+} should be 4.90 μ_B for the high spin configuration in an octahedral crystal field, where the orbital angular moment is quenched. It is possible that the magnetic Mn ions induce spin polarization on the neighbouring Cu sites and thus bring about a larger moment than for a bare Mn ion. This is very similar to the case of subtituent non-magnetic Zn atoms inducing a moment on Cu sites in $La_{1.85}Sr_{0.15}CuO_4$, [19].

A linear variation of the fitted Curie–Weiss temperature with Mn doping content x is found as shown in figure 6. The antiferromagnetic Curie–Weiss temperature rises from -15 to -47 K over the substituted Mn content.

4. Conclusion

In this study, we have investigated the effect of Mn substitution on the structure, resistivity and magnetic properties of the perovskite-related compound $La_4BaCu_5O_{13}$. The structure analysis showed that single-phase samples for $La_4BaCu_{5-x}Mn_xO_{13+\delta}$ can be obtained when

$0 \leqslant x \leqslant 1.5$, and that substitution of Mn for Cu is random. The three levels of Mn-substituted sample studied all exhibit semiconductor-like conduction behaviour. The temperature dependence of resistivity for these samples basically can be described by a 3D VRH conduction process, due to hopping between localized states near the Fermi level. The crossover from metallic transport to semiconductor-like transport with increasing Mn substitution can be attributed to decreasing number and localization of holes induced by Mn. The measurements of the magnetization under a field of 0.5 T indicates there is no magnetic ordering in $La_4BaCu_{5-x}Mn_xO_{13+\delta}$ ($x = 0.5$, 1.0, and 1.5) down to 5 K. Instead, the magnetic susceptibility obeys the Curie–Weiss law better. But probably because the Mn ions induce spin polarization at neighbouring Cu lattice sites, the fitted effective moment from the C–W law is nearly twice the calculated moment for bare Mn^{3+} ions in sixfold coordination.

Acknowledgment

G D Liu gratefully acknowledges discussions with Dr F Zhou.

References

[1] Bednorz J G and Müller K A 1986 *Z. Phys.* B **64** 189
[2] Jorgensen J D 1991 *Phys. Today* **44** 34
[3] Ramirez A P 1997 *J. Phys: Condens. Matter* **9** 8171
[4] Tokura Y 1991 *Physics of High Temperature Superconductors* (Berlin: Springer)
[5] Michael C M, Shirane G, Endoh Y, Hirota K, Moritomo K and Tokura Y 1996 *Phys. Rev.* B **53** 14 285
Jin S, Tiefel T H, McCormack M, Fastnacht R A, Ramesh R and Chen L H 1994 *Science* **264** 413
[6] Zhao G-M, Hunt M B, Keller H and Müller K A 1997 *Nature* **385** 236
[7] Zhao G-M, Conder K, Keller H and Müller K A 1996 *Nature* **381** 676
[8] Xiao Gang, Streitz F H, Gavrin A, Du Y W and Chien C L 1987 *Phys. Rev.* B **35** 35
[9] Hasegawa H, Kisho K, Aoki M, Ooba N, Kitazaw K and Tanaka S 1987 *J. Appl. Phys.* **26** L337
[10] Kochelaev B I, Kan L, Elschner B and Elschner S 1994 *Phys. Rev.* B **49** 3106
[11] Dhingra I, Kashyap S C and Das B K 1994 *J. Mater. Res.* **9** 2771
[12] Saini N L, Srivastava P, Sekhar B R and Garg K B 1992 *Int. J. Mod. Phys.* B **6** 3515
[13] Michel C, Er-Rakho L, Hervieu N, Pannetier J and Raveau B 1987 *J. Solid State Chem.* **68** 143
[14] Michel C, Er-Rakho L and Raveau B 1985 *Mater. Res. Bull.* **20** 667
[15] Mott N F 1990 *Metal–Insulator Transitions* 2nd edn (London: Taylor and Francis)
[16] Shafarman W N, Koon D W and Castner T G 1989 *Phys. Rev.* B **40** 1216
[17] Matsubara I, Funahashi R, Kida N, Ueno K and Ishikawa H 1997 *Physica* C **282–287** 945
[18] Torrance J B, Tokura Y, Nazzal A and Parkin S S P 1988 *Phys. Rev. Lett.* **60** 542
[19] Zagoulaev S, Monod P and Jegoudez J 1996 *Physica* C **259** 271